Gen. Math. Notes, Vol. 33, No. 1, March 2016, pp. 26-39

ISSN 2219-7184; Copyright © ICSRS Publication, 2016
www.i-csrs.org
Available free online at http://www.geman.in

Flow through Variable Permeability Composite Porous Layers

M.S. Abu Zaytoon[1], T.L. Alderson[2] and M.H. Hamdan[3]

[1,2,3]Department of Mathematical Sciences, University of New Brunswick
P.O. Box 5050, Saint John, New Brunswick, Canada, E2L 4L5
[1]E-mail: m.zaytoon@unb.ca
[2]E-mail: tim@unb.ca
[3]E-mail: hamdan@unb.ca

(Received: 20-1-16 / Accepted: 13-3-16)

Abstract

Flow through a variable permeability Brinkman porous layer with quadratic permeability function, underlain by a Darcy porous layer of variable linear permeability function is analysed. The model flow demonstrates the compatibility between the low-order Darcy law and the Brinkman equation in the sense that at the interface between the layers it is possible to impose equality of the non-zero shear stresses. A matching procedure is also introduced for velocity computation near the point of singularity associated with the resulting Cauchy-Euler equation.

Keywords: *Variable Permeability, Darcy-Brinkman Layers.*

1 Introduction

The experiments of Beavers and Joseph, [1], on the flow through a channel over a Darcy porous layer, and their proposing a slip flow condition at the interface, represents the starting point of a large volume of research work devoted to this

problem. Many excellent reviews on the subject matter and applications of this type of flow are available (cf. [3, 8, 16, 17] and the references therein).

In the study of flow through a channel bounded by a Darcy porous layer, a problem arises with the matching condition at the interface between the porous layer and the channel. At the interface, there exists a shear stress discontinuity, a permeability discontinuity, and the low-order of Darcy's law makes it incompatible with the Navier-Stokes equations. This incompatibility causes an apparent slip in the fluid velocity at the assumed sharp interface, and has been handled with the Beavers and Joseph's slip condition, [1], that was intended to interpret the enhancement in the volumetric flow rate in the channel as a result of introducing a porous boundary. Conditions at the interface between a channel and a porous layer are important as they influence mass and heat transfer in the flow domain. This initiated a need for a non-Darcy model to govern the flow in the porous layer, and to be compatible with the Navier-Stokes equations.

While much research has been devoted to the analysis of conditions at the interface between a channel and a porous medium and the types of governing equations that are best suited for the flow through the porous layer, [3, 4, 10, 12, 14, 15, 16, 17], recent advances in the field deal with flow through variable permeability layers, [2, 5, 6, 7, 9, 13], and the analysis of the transition layer that is associated with Brinkman's equation and proposed by Nield and Koznetsov, [11].

Brinkman's equation with variable permeability, [7], has been of great utility in the analysis of a transition layer between a Darcy porous layer and a channel through which the flow is governed by Navier-Stokes equations, [11]. However, most of the work carried out on analysis of flow in the transition layer has assumed a Brinkman layer with variable permeability underlain by a constant permeability Darcy layer. Little to no work has provided analysis of the problem of variable permeability porous layer bounding a Brinkman layer of variable permeability. This gives rise to the current work in which we provide analysis of the more general situation wherein the Darcy layer is of variable permeability in order to capture naturally occurring porous layers of different permeability. We do not consider the Brinkman layer as a transition layer in this work; rather, we consider flow through a two-layer composite configuration, shown in **Fig. 1**, one Darcy and one Brinkman layer, both possessing variable permeability and both bounded by solid, impermeable walls on opposite sides. The common side between layers is an assumed sharp interface on which we will assume permeability, velocity, and shear stress continuity.

2 Problem Formulation

Consider the steady, unidirectional flow of a viscous fluid through the porous layers shown in **Fig. 1**, and termed Darcy layer (the lower porous layer where Darcy's law is valid) and Brinkman layer (the upper porous layer where

Brinkman's equation is valid). Flow in both layers is driven by the same constant pressure gradient, and each layer is of variable permeability. The layers are bounded by solid, impermeable walls at $y = -D$ and at $y = D$, and the interface between the layers is an assumed sharp interface, located at $y = 0$.

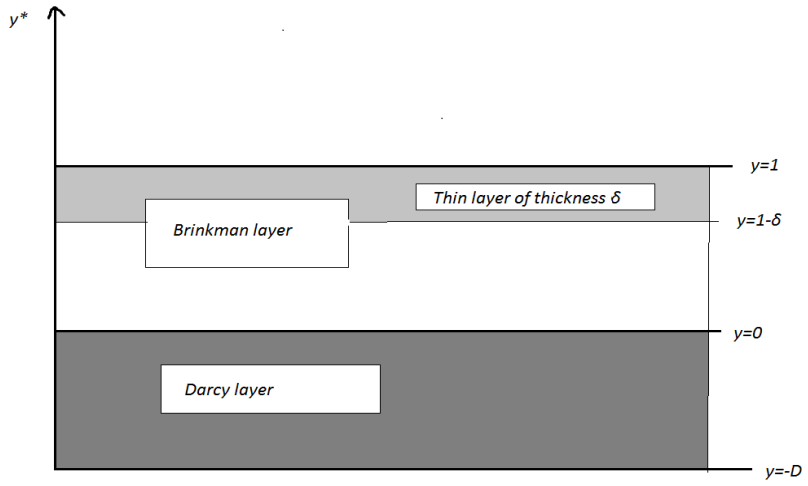

Fig. 1: Representative Sketch

In the upper layer, $0 < y < D$, the flow is governed by Brinkman's unidirectional flow equation

$$\frac{d^2u}{dy^2} - \frac{1}{\vartheta k_2(y)}u = Q \qquad ...(1)$$

and in the lower layer, $-D < y < 0$, the flow is governed by Darcy's unidirectional flow equation

$$v = Rk_1(y) \qquad \ldots(2)$$

where $Q = \frac{p_x}{\mu_{eff}}$, $R = -\frac{p_x}{\mu}$, $\vartheta = \frac{\mu_{eff}}{\mu}$, $p_x < 0$ is the constant pressure gradient, μ is the fluid viscosity coefficient, and μ_{eff} is the effective viscosity of fluid in the Brinkman layer, $k_1(y)$ is the variable permeability in the Darcy layer, and $k_2(y)$ is the variable permeability in the Brinkman layer. Equations (1) and (2) are to be solved subject to the following conditions:

Conditions at the interface, y = 0, are the following velocity continuity, permeability continuity, and continuity of the normal component of shear stress, respectively,

$$u(0) = v(0), k_1(0) = k_2(0), \vartheta \frac{du}{dy}(0) = \frac{dv}{dy}(0). \quad \ldots(3)$$

Conditions at the solid walls are the no-slip conditions and vanishing permeability, respectively, namely

$$u(D) = 0, v(-D) = 0, k_1(-D) = 0, k_2(D) = 0. \quad \ldots(4)$$

3 Method of Solution

Assume that the permeability $k_1(y)$ in the Darcy layer to be an increasing linear function of y, that reaches a maximum value, $k_{\max}$, at $y = 0$, and in the Brinkman layer a quadratic permeability function, $k_2(y)$, written as

$$k_1(y) = \frac{(D+y)k_{\max}}{D} \text{ and } k_2(y) = (a+by)^2 \quad \ldots(5)$$

then the velocity profile in the Darcy layer is obtained from (2) as

$$v(y) = R\frac{(D+y)k_{\max}}{D} \quad \ldots(6)$$

and a shear stress in the lower layer and at the interface given by

$$\frac{dv}{dy} = R\frac{k_{\max}}{D}. \quad \ldots(7)$$

Condition (3) thus yields the following expression for velocity at the interface:

$$u(0) = v(0) = u_i = Rk_{\max}. \quad \ldots(8)$$

Using (3) and (4) gives Brinkman permeability function:

$$a = \mp\sqrt{k_{\max}}, \; b = -\frac{a}{D} = \pm\frac{\sqrt{k_{\max}}}{D} \text{ and } k_2(y) = (\mp\sqrt{k_{\max}} \pm \frac{\sqrt{k_{\max}}}{D}y)^2 . \quad \ldots(9)$$

Choosing $k_2(y) = (\sqrt{k_{\max}} - \frac{\sqrt{k_{\max}}}{D}y)^2$ and letting $Y = 1 - \frac{y}{D}$, equation (1) is transformed into the Cauchy-Euler inhomogeneous ordinary differential equations

$$Y^2 \frac{d^2u}{dY^2} - \frac{D^2}{\vartheta k_{\max}} u = QD^2Y^2. \qquad \ldots(10)$$

General solution to (10) is given by

$$u = c_1\left[1-\frac{y}{D}\right]^{m_1} + c_2\left[1-\frac{y}{D}\right]^{m_2} + C\left[1-\frac{y}{D}\right]^2. \qquad \ldots(11)$$

Where

$$m_1 = \frac{1+\sqrt{1+4\dfrac{D^2}{\vartheta k_{\max}}}}{2},\ m_2 = \frac{1-\sqrt{1+4\dfrac{D^2}{\vartheta k_{\max}}}}{2},\ C = \frac{QD^2}{(2-m_1)(1+m_1)} \qquad \ldots(12)$$

and c_1 and c_2 are determined using conditions (3) and (4) and take the values:

$$c_1 = \frac{Rk_{\max}[m_2 + \frac{1}{\vartheta}] + C[2-m_2]}{[m_2 - m_1]} \text{ and } c_2 = \frac{Rk_{\max}[m_1 + \frac{1}{\vartheta}] + C[2-m_1]}{[m_1 - m_2]}. \qquad \ldots(13)$$

Shear stress in the upper layer is obtained from (11) and takes the form

$$u'(y) = -\frac{c_1 m_1}{D}\left[1-\frac{y}{D}\right]^{m_1-1} - \frac{c_2 m_2}{D}\left[1-\frac{y}{D}\right]^{m_2-1} - \frac{2C}{D}\left[1-\frac{y}{D}\right] \qquad \ldots(14)$$

and has the following value at the interface, y = 0:

$$\frac{du}{dy}(0) = -\frac{c_1 m_1}{D} - \frac{c_2 m_2}{D} - \frac{2C}{D}. \qquad \ldots(15)$$

Solution to the given problem is thus completely determined and can be expressed in dimensionless form using the following dimensionless variables:

$$y^* = \frac{y}{D}; u^* = \frac{\mu u}{(-p_x)D^2}; v^* = \frac{\mu v}{(-p_x)D^2}; k_i^*(y) = \frac{k_i(y)}{D^2} = k_i^*(y^*D) = k_i^*(y^*);$$
$$k^*_{\max} = \frac{k_{\max}}{D^2}. \qquad \ldots(16)$$

The dimensionless porous layers span the following dimensionless length y^*: Darcy layer: $-1 \le y^* \le 0$ and $0 \le y^* \le 1$ for Brinkman layer. Dimensionless

velocity profiles in the Brinkman and Darcy layers are given by the following equations, respectively

$$u^* = \left\{ \frac{k^*_{\max}[\vartheta m^*_2 + 1]}{\vartheta[m^*_2 - m^*_1]} + \frac{1}{\vartheta(m^*_1 - 2)[m^*_2 - m^*_1]} \right\} \left[1 - y^*\right]^{m^*_1}$$
$$+ \left\{ \frac{k^*_{\max}[\vartheta m^*_1 + 1]}{\vartheta[m^*_1 - m^*_2]} + \frac{1}{\vartheta(m^*_2 - 2)[m^*_1 - m^*_2]} \right\} \left[1 - y^*\right]^{m^*_2} - \left\{ \frac{1}{\vartheta(2 - m^*_1)(2 - m^*_2)} \right\} \left[1 - y^*\right]^2 \quad \ldots(17)$$

$$v^* = k^*_1(y^*) = k^*_{\max}(1 + y^*). \quad \ldots(18)$$

$$m^*_1 = \frac{1 + \sqrt{1 + \frac{4}{\vartheta k^*_{\max}}}}{2} \text{ and } m^*_2 = \frac{1 - \sqrt{1 + \frac{4}{\vartheta k^*_{\max}}}}{2}. \quad \ldots(19)$$

Dimensionless permeability distributions in the lower and upper layers are given respectively by

$$k^*_1(y) = k^*_{\max}(1 + y^*) \text{ and } k^*_2(y^*) = k^*_{\max}(1 - y^*)^2 \quad \ldots(20)$$

while the dimensionless velocity and shear stress at the interface are given, respectively, by

$$u_i^* = k^*_{\max} \quad \ldots(21)$$

$$\frac{du^*}{dy^*}(0) = \frac{k^*_{\max}}{\vartheta}. \quad \ldots(22)$$

4 Results and Discussion

The dimensionless equations (17) to (22), above, are dependent on the parameters $k^*_{\max}$ and ϑ. The parameter $\vartheta = \frac{\mu_{eff}}{\mu}$ is the ratio of effective viscosity to the fluid viscosity. In the absence of concrete experimental or theoretical evidence supporting its value, we will take the full range of values $\vartheta = 0.5$, 0.95, 1, 1.05, and 1.5. The parameter $k^*_{\max}$ is the dimensionless permeability at the interface. It is in fact the dimensionless Darcy number, *Da*, which has a maximum value of unity. In this analysis we take the following range of values for $k^*_{\max}$: 1, 0.1, 0.01, 0.001, 0.0001, and 0.00001.

Using the above values of $k^*_{\max}$ and ϑ, we provide the following data for velocity and shear stress at the interface, velocity profiles, and permeability distributions in the layers.

4.1 Velocity and Shear Stress at the Interface

Equation (21) provides an expression for the dimensionless velocity u_i^* at the interface in terms of the dimensionless permeability $k^*_{\max}$. It is clear and expected that as $k^*_{\max}$ decreases, the dimensionless velocity at the interface decreases. Furthermore, this dimensionless velocity is independent of ϑ. Dependence of the dimensional velocity at the interface on viscosity, pressure gradient and on the dimensional permeability at the interface is given by equation (8), or $u_i = -\frac{p_x}{\mu} k_{\max}$, which shows its increase with increasing permeability and magnitude of pressure gradient, and its decrease with increasing fluid viscosity, μ. For a given μ_{eff}, an increase in μ results in a decrease in ϑ. We can then conclude that the dimensional velocity at the interface decreases with decreasing ϑ.

Equation (21) gives an expression for the dimensionless normal component of velocity derivative at the interface. While the expression $\vartheta \frac{du^*}{dy^*}(0)$ is given by $k^*_{\max}$, hence has the same values as the dimensionless velocity at the interface, its dimensional expression shows its dependence on the pressure gradient, fluid viscosity and depth of the lower porous layer. Magnitude of this term is inversely proportional to the depth of the lower porous layer. In fact, in the limit as *D* approaches infinity, shear stress at the interface approaches zero (the value of shear stress at the interface as given by Darcy's law with constant permeability).

4.2 Dimensionless Permeability Distribution

Equation (20) gives the expressions of the dimensionless permeability distributions in the Darcy and Brinkman layers, respectively. The linear profile starts at zero on the lower bounding wall, and increases till it reaches $k^*_{\max}$ at the interface. In the upper layer, the dimensionless permeability profile is parabolic with a maximum value at the interface and falls to zero on the upper boundary. Graphs of the two permeability profiles are shown in **Figure 2** for the range of $k^*_{\max}$ (Darcy number) of 0.1 and 1.

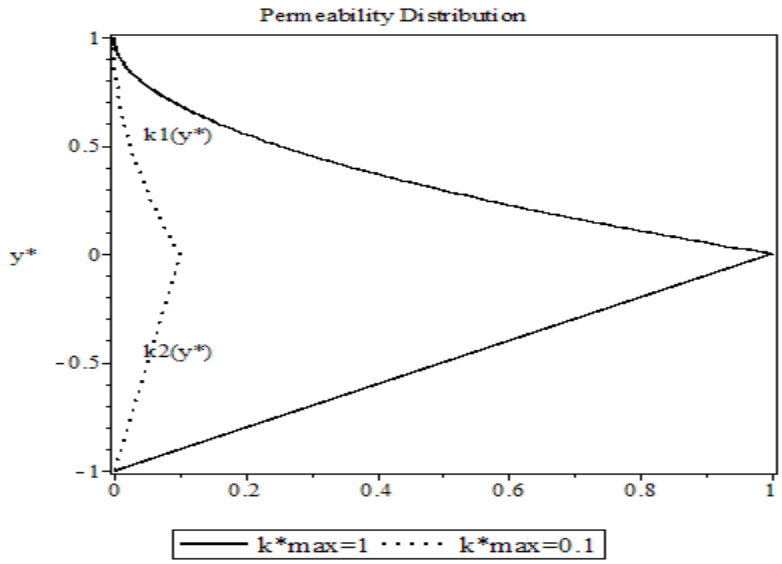

Fig. 2: Permeability Distribution in the Two Layers

4.3 Velocity Profiles in the Porous Layers

Dimensionless velocity profiles in the upper and lower layers are given, respectively, by equations (17) and (18). While the profile in the lower layer is dependent on $k^*_{\max}$, the profile in the upper layer depends on both $k^*_{\max}$ and ϑ. The values of the velocity in the upper layer become asymptotically large as we get close to the upper boundary. Inherent in the Cauchy-Euler equation is the ordinary point of singularity (zero of the coefficient of the highest derivative). Boundary conditions do not remove this singularity. Therefore, solution is valid near the point of singularity. We therefore follow the steps below to generate velocity values near the upper wall. Taking the limit of u^* as $y^* \to 1^-$, we obtain:

$$\lim_{y^*\to 1^-} u = 0 = c_1 \lim_{y^*\to 1^-} \left[1-y^*\right]^{m_1} + c_2 \lim_{y^*\to 1^-} \frac{1}{\left[1-y^*\right]^{-m_2}} + \lim_{y^*\to 1^-} C\left[1-y^*\right]^2 . \qquad \ldots(23)$$

Noting that $\lim_{y^*\to 1^-} \left[1-y^*\right]^{m_1} = 0$, $\lim_{y^*\to 1^-} C\left[1-y^*\right]^2 = 0$ and $\lim_{y^*\to 1^-} \frac{1}{\left[1-y^*\right]^{-m_2}} = +\infty$,

We need

$c_2 \lim_{y^*\to 1^-} \frac{1}{\left[1-y^*\right]^{-m_2}} \to 0$, or $c_2 = 0$.

Therefore, near $y^* = 1$, we have $u = c_1\left[1-y^*\right]^{m_1} + C\left[1-y^*\right]^2$. …(24)

Velocity computations thus proceed as follows:

1) Use equation (17) to calculate the velocity up to the edge of boundary layer.
2) Use equation (24) to calculate the velocity from the edge of boundary layer to the upper boundary.

In order to calculate the limits of the boundary layer, we use definition of the boundary layer thickness, δ, as square root of the permeability, namely

$$\delta = \sqrt{k^*{}_2(y^*)} = \sqrt{k^*{}_{\max}}(1-y^*). \qquad \ldots(25)$$

Now, $y^* \geq \delta \Rightarrow y^* \geq \sqrt{k^*{}_{\max}}(1-y^*) = \sqrt{k^*{}_{\max}} - y^*\sqrt{k^*{}_{\max}}$ or

$y^*(1+\sqrt{k^*{}_{\max}}) \geq \sqrt{k^*{}_{\max}}$.

Hence $y^* \geq \dfrac{\sqrt{k^*{}_{\max}}}{(1+\sqrt{k^*{}_{\max}})}$. $\qquad \ldots(26)$

Critical values of y^* for different $k^*{}_{\max}$ are listed in **Table 1** below. Therefore, we use equation (17) to calculate the velocity up to the critical value of y^*, and equation (24) to calculate the velocity for $y^* < y < 1$.

Table 1: Critical Values of y^* for different $k^*{}_{\max}$

$k^*{}_{\max}$	critical y^* (inequality (26))	$\delta = \sqrt{k^*{}_{\max}}(1-y^*)$
1	0.5	0.5
0.1	0.2402	0.2402
0.01	0.0909	0.0909
0.001	0.0306	0.0306
0.0001	0.0099	0.0099

While the above decomposition of the flow domain seems reasonable it does however result in a jump in the velocity at $y = \dfrac{\sqrt{k^*{}_{\max}}}{(1+\sqrt{k^*{}_{\max}})}$, as can be seen in **Figs. 3** and **4**, below, which illustrate the velocity profiles for $\vartheta = 1$ and different

values of $k^*_{\max}$ .This points to the need for matching the two solutions at the point of jump discontinuity, as explained below.

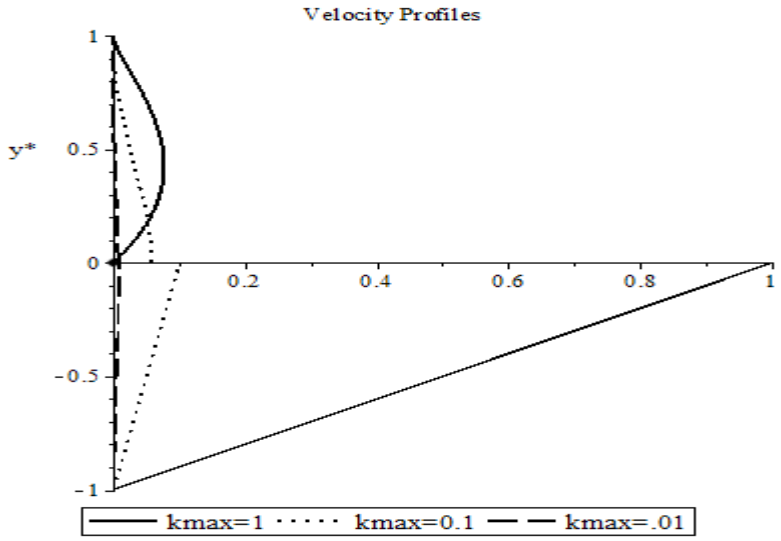

Fig. 3: Velocity Profiles $u^*(y), v^*(y)$, for $\vartheta = 1$and different values of $k^*_{\max}$.

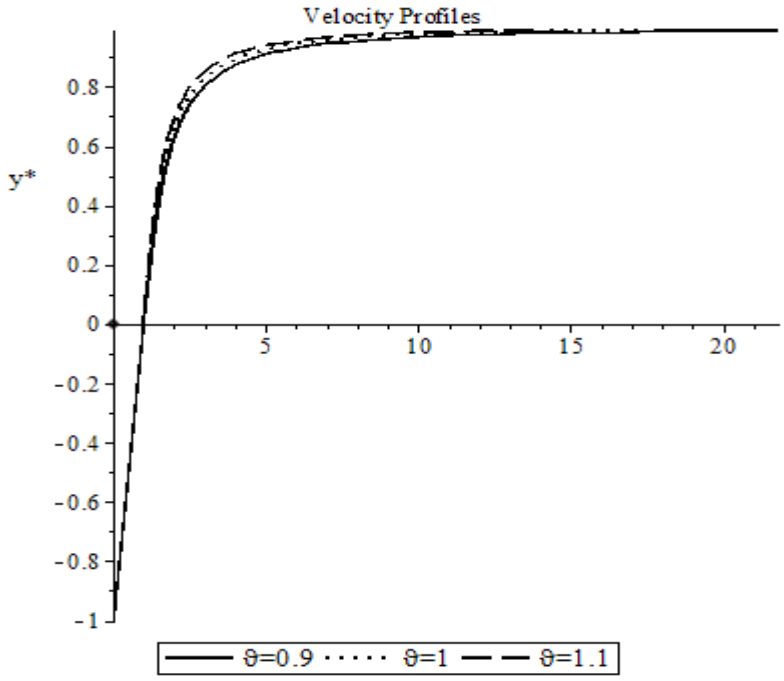

Fig. 4: Velocity Profiles $u^*(y), v^*(y)$, for $k^*_{\max}$ =1, and different values of ϑ

Figure 1 represents the matching configuration and illustrates three regions in the flow domain: the lower region where Darcy's law is valid; the middle region where Brinkman's equation and its solution, given by equation (17), are valid, and the boundary layer region which in which equation (24) is valid. We can thus state the velocity profile in the Brinkman layer as follows:

$$u^* = u_1^* = B_1\left[1-y^*\right]^{m^*_1} + B_2\left[1-y^*\right]^{m^*_2} - B_3\left[1-y^*\right]^2, \quad \text{when } 0 < y < 1-\delta \qquad \ldots(27)$$

$$u^* = u_2^* = B_1\left[1-y^*\right]^{m^*_1} - B_3\left[1-y^*\right]^2, \quad \text{when } 1-\delta < y < 1. \qquad \ldots(28)$$

Where

$$B_1 = \left\{\frac{k^*_{\max}[\vartheta m^*_2 + 1]}{\vartheta[m^*_2 - m^*_1]} + \frac{1}{\vartheta(m^*_1 - 2)[m^*_2 - m^*_1]}\right\} \qquad \ldots(29)$$

$$B_2 = \left\{\frac{k^*_{\max}[\vartheta m^*_1 + 1]}{\vartheta[m^*_1 - m^*_2]} + \frac{1}{\vartheta(m^*_2 - 2)[m^*_1 - m^*_2]}\right\} \qquad \ldots(30)$$

$$B_3 = \left\{\frac{1}{\vartheta(2-m^*_1)(2-m^*_2)}\right\}. \qquad \ldots(31)$$

Now, for velocity continuity at $y = 1-\delta$ we must match u_2^* with u_1^* by letting

$$u_2^* = B_1\left[1-y^*\right]^{m^*_1} - A\left[1-y^*\right]^2, \quad \text{when } 1-\delta < y < 1 \qquad \ldots(32)$$

And

$$u_1^*(1-\delta) = u_2^*(1-\delta). \qquad \ldots(33)$$

Equations (27)-(33) yield

$$A = B_2 - B_3\delta^{m^*_2-2} \qquad \ldots(34)$$

$$u_2^* = B_1\left[1-y^*\right]^{m^*_1} - (B_2 - B_3\delta^{m^*_2-2})\left[1-y^*\right]^2 \quad \text{when } 1-\delta < y < 1. \qquad \ldots(35)$$

Now, using (27) and (35), we plot the velocity profiles in the upper layer. In Figures 5 and 6 we illustrate the velocity profile in both layers for $k^*_{\max} = 0.1$ and 1, and $\vartheta = 1$. These graphs show the expected decrease in the velocity in the upper layer as we move away from the interface, and the continuity of velocity at the edge of boundary layer.

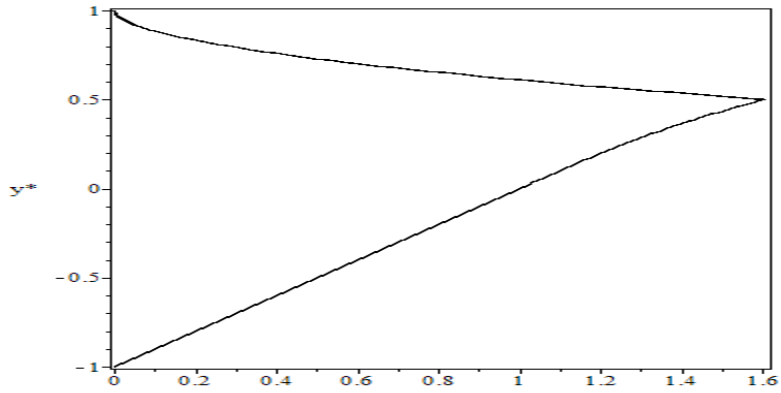

Fig. 5: Matched Velocity profiles for $k^*_{\max} = 1, \vartheta = 1$

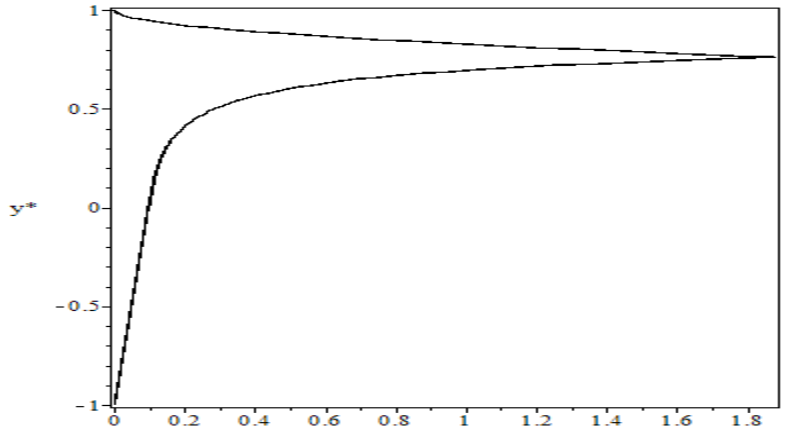

Fig. 6: Matched Velocity profiles for $k^*_{\max} = 0.1, \vartheta = 1$

5 Conclusion

In this work we considered the flow of a viscous fluid through a two-layer configuration. The flow through one layer is governed by Darcy's law with variable permeability, and the other by a Brinkman's equation with quadratic variable permeability. Brinkman's equation reduces to a Cauchy-Euler equation. Solution to this equation becomes excessively large for small values of dimensionless maximum permeability. To remedy the arising jump discontinuity in the velocity as we approach the upper boundary, we devised a matching condition that induces velocity continuity at the edge of the boundary layer to the upper solid boundary.

References

[1] B. Alazmi and K. Vafai, Analysis of variants within the porous media transport models, *J. Heat Transfer*, 122(2000), 303-326.

[2] G.S. Beavers and D.D. Joseph, Boundary conditions at a naturally permeable wall, *J. Fluid Mech.*, 30(1967), 197-207.

[3] M. Chandesris and D. Jamet, Boundary conditions at a fluid-porous interface: An a priori estimation of the stress jump boundary conditions, *Int. J. Heat Mass Transfer*, 50(2007), 3422-3436.

[4] B.C. Chandrasekhara, K. Rajani and N. Rudraiah, Effect of slip on porous-walled squeeze films in the presence of a magnetic field, *Appl. Scientific Res.*, 34(1978), 393-411.

[5] A.H.D. Cheng, Darcy's flow with variable permeability: A boundary integral solution, *Water Resour. Res.*, 20(1984), 980-984.

[6] M. Ehrhardt, *An Introduction to Fluid-Porous Interface Coupling*, Weierstrass Institute for Applied Analysis and Stochastics, Berlin, Germany, (2010).

[7] M.H. Hamdan and M.T. Kamel, Flow through variable permeability porous layers, *Adv. Theor. Appl. Mech.*, 4(2011), 135-145.

[8] M. Kaviany, Laminar flow through a porous channel bounded by isothermal parallel plates, *Int. J. Heat Mass Transfer*, 28(1985), 851-858.

[9] M.S. Mahmoud and H. Deresiewicz, Settlement of inhomogeneous consolidating soils- I: The single-drained layer under confined compression, *Int. J. Numer. Anal. Methods Geomech*, 4(1980), 57-72.

[10] G. Neale and W. Nader, Practical significance of Brinkman's extension of Darcy's law: Coupled parallel flows within a channel and a bounding porous medium, *Canadian J. Chem. Eng.*, 52(1974), 475-478.

[11] D.A. Nield and A.V. Kuznetsov, The effect of a transition layer between a fluid and a porous medium: Shear flow in a channel, *Transport in Porous Media*, 78(2009), 477-487.

[12] J.A. Ochoa-Tapia and S. Whitaker, Momentum jump condition at the boundary between a porous medium and a homogeneous fluid: Inertial effects, *J. Porous Media*, 1(1981), 201-217.

[13] M. Parvazinia, V. Nassehi, R.J. Wakeman and M.H.R. Ghoreishy, Finite element modelling of flow through a porous medium between two parallel plates using the Brinkman equation, *Transport in Porous Media*, 63(2006), 71-90.

[14] N. Rudraiah, Flow past porous layers and their stability, *Encyclopedia of Fluid Mechanics*, Slurry Flow Technology, Gulf Publishing, Chapter 14(1986), 567-647.

[15] P.G. Saffman, On the boundary condition at the surface of a porous medium, *Studies in Applied Mathematics*, L(1971), 93-101.

[16] M. Sahraoui and M. Kaviany, Slip and no-slip velocity boundary conditions at interface of porous, plain media, *Int. J. Heat Mass Transfer*, 35(1992), 927-943.

[17] K. Vafai and R. Thiyagaraja, Analysis of flow and heat transfer at the interface region of a porous medium, *Int. J. Heat and Mass Transfer*, 30(1987), 1391-1405.